

**$X(3872) \rightarrow J/\psi \gamma$  decay in the  $D\bar{D}^*$  molecular picture**

F. Aceti, R. Molina, and E. Oset

*Departamento de Física Teórica and IFIC, Centro Mixto Universidad de Valencia-CSIC, Institutos de Investigación de Paterna, Apartado 22085, 46071 Valencia, Spain*

(Received 31 July 2012; published 17 December 2012)

From a picture of the  $X(3872)$  where the resonance is a bound state of  $\bar{D}D^* - c.c.$ , we evaluate the decay width into the  $J/\psi \gamma$  channel, which is sensitive to the internal structure of this state. For this purpose we evaluate the loops through which the  $X(3872)$  decays into its components, and the  $J/\psi$  and the photon are radiated from these components. We use the local hidden gauge approach extrapolated to  $SU(4)$  with a particular  $SU(4)$  breaking. The radiative decay involves anomalous couplings, and we obtain acceptable values which are compared to experiments and results of other calculations. Simultaneously, we evaluate the decay rate for the  $X(3872)$  into  $J/\psi \omega$  and  $J/\psi \rho$ , and the results obtained for the ratio of these decay widths are compatible with the experiment. We also show that considering only the  $\bar{D}^0 D^{*0} - c.c.$  component in the radiative decay reduces the partial decay width in more than three orders of magnitude, in large discrepancy with experiment.

DOI: [10.1103/PhysRevD.86.113007](https://doi.org/10.1103/PhysRevD.86.113007)

PACS numbers: 13.40.Hq, 14.40.Pq, 14.40.Rt

**I. INTRODUCTION**

The first observation of the  $X(3872)$  decay into  $J/\psi \gamma$  was reported by the BELLE Collaboration in Ref. [1]. Later on, this decay mode was confirmed by the BABAR Collaboration in Ref. [2] and more recently again in BELLE in Ref. [3]. Theoretically, this decay mode had already received some early attention and was studied in Refs. [4–7], assuming either a charmonium state or a molecular state. A thorough discussion of the different models used and the results can be seen in Ref. [8], which has also been updated recently in Ref. [9]. A recent work assuming the  $X(3872)$  to be a charmonium state is presented in Ref. [10] and assuming it to be a tetraquark in Ref. [11]. In Ref. [12] it is assumed to be a mixture of a charmonium and a molecular component, and using QCD sum rules, a good rate is obtained for the  $J/\psi \gamma$  decay mode versus the  $J/\psi \pi^+ \pi^-$  one, which is evaluated in Ref. [13]. In Ref. [8] the authors consider, like in the work of Braaten and Kusunoki [5], the  $X(3872)$  resonance to be a molecule of  $D^0 \bar{D}^{*0} - c.c.$ , as in Ref. [14], and in addition, they include the possibility of a  $c\bar{c}$  admixture. In Ref. [8] an effective Lagrangian is postulated to provide the coupling of the  $X(3872)$  to the  $D^0 \bar{D}^{*0}$  components, with an unknown wave function. The effective coupling needed in the loops for radiative decay of the  $X(3872)$  is obtained using the Weinberg compositeness condition [15,16], reformulated in Ref. [17] as  $g^2 = -(\frac{\partial}{\partial s} G)^{-1}$ , where  $G$  is the loop function of the  $D^0$  and  $\bar{D}^{*0}$  propagators. The procedure has been shown to provide a fair description of the molecular states in other works [18–20]. The results of Dong *et al.* [8] are tied to unknowns on the regularization of the loop functions, the  $\Lambda_M$  parameter used in Ref. [8], the coupling to the  $c\bar{c}$  component, and the binding. The results obtained for

the  $X(3872)$  decay into the  $J/\psi \gamma$  channel are of about 125–250 keV, taking reasonable values for the  $\Lambda_M$  parameter between 2 and 3 GeV.

In Ref. [9] the authors include the charge components of  $D^+ D^{*-} - c.c.$ , which were found necessary to explain the ratio of  $X(3872)$  to  $J/\psi \rho$  and  $J/\psi \omega$  in Refs. [17,21] (see further developments in this direction in Ref. [22]). The novelty with respect to the previous work of Dong *et al.* [8] is that the authors use a smaller  $\Lambda_M$  cutoff, of the order of 0.5 GeV, to regularize the loop function, such that the wave function of the  $D^0 \bar{D}^{*0} - c.c.$  is much more extended in space. The final results of the new evaluations differ quantitatively from those of Dong *et al.* [8] and are now in the range of 2–17 keV. It is then clear that a more systematic approach to the problem has to be done if one wishes to obtain accurate numbers from the molecular picture of the  $X(3872)$ . This is the purpose of the present paper.

A dynamical picture of the  $X(3872)$  in the coupled channels of  $D\bar{D}^* - c.c.$  was elaborated in Ref. [21] using an extrapolation to  $SU(4)$  of chiral Lagrangians used in the study of pseudoscalar meson interaction with vector mesons [23]. This is equivalent to extending to  $SU(4)$  the local hidden gauge approach of [24–27] with a particular  $SU(4)$  breaking. Given the subtlety of the small binding for the neutral  $D^0 \bar{D}^{*0} - c.c.$  component versus the about 7-MeV binding for the charged  $D^+ D^{*-} - c.c.$  components, a coupled channel approach considering these explicit channels with their exact mass, and not assuming isospin symmetry, was done in Ref. [28], concluding that the couplings of the resonance to the neutral and charged components are very similar, which tells us that in strong processes the  $X(3872)$  behaves as a rather good  $I = 0$  object. The  $D_s^+ D_s^{*-} - c.c.$  components

were also included in Refs. [21,28], and we include them here too.<sup>1</sup>

In the present work we follow the approach of [17,28], where all the couplings are determined from the unitary coupled channel approach and are tied to the binding of the  $X(3872)$ , which is generated dynamically as a composite state of  $D\bar{D}^*$  in this picture, but we update these couplings considering the latest results for the masses of particles. The mechanisms for radiative decay are then basically the same as in Ref. [9], except that we also have contributions from the  $D_s\bar{D}_s^*$  components and have, although not many, different couplings of the resonance to the neutral and charged  $D\bar{D}^*$  components. The work is also technically different. The use of wave functions with an arbitrary-size parameter is what regularizes the loops in Ref. [9]. Our work has a different approach to the regularization of the loops, and most of the terms are shown to be convergent. Some terms are formally divergent, but we can isolate the divergence into a term proportional to the same loop function  $G$  which appears in scattering. The function  $G$  is regularized in the scattering problem in order to fit the position of the resonance, so when it comes to evaluate the radiative decay, it is already fixed. Even then, there is still the possibility that a new vertex of the radiative decay loop function introduces a cutoff of longer range ( $\Lambda$  smaller in a momentum cutoff) which introduces extra uncertainties, but we investigate them and find them small.

Traditionally the  $X(3872)$  could be considered as a  $J^P = 1^{++}$  or  $J^P = 2^{-+}$  state, and there is a work similar to the one of Dong *et al.* [9] but assuming  $J^P = 2^{-+}$  [30]. Here we will continue to use the  $J^P = 1^{++}$ , which is supported by recent analysis of data in Refs. [31,32].

Our work proceeds as follows: in the next section we present the formalism for the work with the Feynman diagrams used and the scheme to evaluate them. In Sec. III we present the results for  $X(3872) \rightarrow J/\psi\gamma$ ,  $J/\psi\omega$ ,  $J/\psi\rho$  and compare them to the experiment, discussing the role of the charged components of the  $X(3872)$  wave function. In Sec. IV we summarize our results.

## II. FORMALISM

### A. Brief summary of the model used for $D\bar{D}^*$ interaction

In Refs. [21,33], the interaction between pseudoscalars and vector mesons is studied including the charm sector. The

<sup>1</sup>We should recall that in any field theory one always selects some channels and ignores others. The ignorance of some channels can be coped with by introducing counterterms in the theory, then losing predicting power for some processes, but they can serve to study other processes where the counterterms are negligible. One does not know this *a priori*, but in principle the explicit consideration of close-by channels renders the theory more predictive than if they were ignored. One example of this can be found in the study of the scattering of  $D$  and  $D^*$  mesons off the  $X(3872)$  as done in Ref. [29], where the  $D\bar{D}^{*0}$  component is by far dominant.

potential is like the Weinberg-Tomozawa interaction between pseudoscalar mesons but including the vector meson fields [23]. In Refs. [21,28], all the different currents within the  $SU(4)$  scheme are classified in terms of  $SU(3)$  currents, and the breaking symmetry parameters are introduced to account for the suppression of the heavy meson exchange.<sup>2</sup> Within this formalism, the  $X(3872)$  is a dynamically generated resonance from the interaction of  $D\bar{D}^*$ , having an eigenstate of positive  $C$  parity with isospin  $I = 0$ . It also has some component of  $D_s\bar{D}_s^*$ . In fact, the basis of positive  $C$  parity and  $I = 0$  for these two channels corresponds to

$$\begin{aligned} & \frac{1}{\sqrt{2}} |(D^*\bar{D} - \bar{D}^*D), I = 0, I_3 = 0\rangle \\ &= \frac{1}{2} |(D^{*+}D^- - D^{*-}D^+ + D^{*0}\bar{D}^0 - \bar{D}^{*0}D^0)\rangle \\ & \frac{1}{\sqrt{2}} |(D_s^*\bar{D}_s - \bar{D}_s^*D_s), I = 0, I_3 = 0\rangle \\ &= \frac{1}{\sqrt{2}} |(D_s^{*+}D_s^- - D_s^{*-}D_s^+)\rangle. \end{aligned} \quad (1)$$

The method employed in Ref. [21] is a fully unitary approach solving the Bethe-Salpeter equations in coupled channels. The on-shell factorized form of these equations is used, providing a structure of the amplitude like the one of a renormalized theory described in the Appendix of Ref. [35] [see Eq. (A2)] but not restricted to energies close to threshold. Indeed in Refs. [36,37], it was explicitly shown how the terms tied to the off-shell part of the potentials could be absorbed into renormalized parameters of the theory. Alternatively, using the  $N/D$  method and dispersion relations, in Refs. [38,39] the same results were obtained with the resulting amplitude in matrix form for the coupled channels

$$T^{-1} = (V^{-1} - G), \quad (2)$$

where  $V$  is the kernel of the interaction, that we call potential, and  $G$  is the loop function for the four-dimensional integral of two mesons propagator

$$\begin{aligned} G(P = p + k) &= i \int \frac{d^4q}{(2\pi)^4} \frac{1}{q^2 - m_p^2 + i\epsilon} \\ &\times \frac{1}{(p + k - q)^2 - m_V^2 + i\epsilon}, \end{aligned} \quad (3)$$

diagonal in the coupled channel space. This integral is conveniently regularized with a cutoff in the three

<sup>2</sup>Concerning the use of the  $SU(4)$  treatment of Gamermann and Oset [28], we would like to refer the reader to Sec. II D of Ref. [34], where a thorough discussion on this issue is given, providing arguments in favor of its use and also showing the limitations. In the present case we could just invoke  $SU(3)$  symmetry to relate the potentials, or the couplings, and finally impose the Weinberg compositeness condition in coupled channels, Eq. (4), to determine the couplings.

momentum or using dimensional regularization. The latter means that the integral is calculated for  $d = 4 + \eta$  and  $\eta \rightarrow 0$  after making a subtraction. The procedure is equivalent to using a subtraction in the dispersion relation of the  $N/D$  method used in Refs. [38,39]; the equivalence of both methods was established in Refs. [39,40].

The potential used in Refs. [21,28] is a contact potential, since it is based on the exchange of vector mesons from the perspective of the local hidden gauge formalism, and due to the large mass of the vector mesons, their propagators are effectively replaced by constants.<sup>3</sup>

Different approaches have been used in the literature, and one of them is pion exchange [41–49]. The way to treat pion exchange differs from one approach to another, and so do the results and the conclusions. A review of those works is given in Ref. [50], where a thorough study of the issue is done, considering the coupled channels  $DD^*$ ,  $\bar{D}D^*$ , and  $DD\pi$ . It is shown there that a short range  $DD^* \rightarrow DD^*$  contact term is needed to arrive at well-defined equations, with its strength tied to the regulator needed to make the theory convergent. Because of this ambiguity, it was concluded there that no model-independent statement can be made on the importance of the one pion exchange in the formation of the  $X(3872)$ . However, with respect to what concerns us here, a relevant finding in Ref. [50] is that the  $X(3872)$  coupling to the  $D^0\bar{D}^{*0}$  component is weakly dependent on the kind of pion dynamics included.

Actually, in a different approach and a similar problem, the interaction of  $D^*\bar{D}^*$  mesons leading to  $X$ ,  $Y$ ,  $Z$  molecules, the  $\pi$  exchange is explicitly taken into account by means of a box diagram that eliminates all possible ambiguities tied to the possibility of having the pion on shell [51]. There it was found that the corrections to the amplitudes induced by the  $\pi$ -exchange driven box diagram were very small, using cutoffs or form factors of reasonable size for the effective theories.

The Weinberg compositeness condition is very accurate to determine the coupling, and for a binding of the  $D^0\bar{D}^{*0}$  channel below 1 MeV, as is the case here, the results with a contact potential or with the dynamical pion are practically indistinguishable.

With the  $DD^*$  coupling under control, a model is needed to obtain the coupling to the charged  $D^+D^{*-}$  – c.c. or charmed-strange  $D_s^+D_s^{*-}$  – c.c. components, and for this we use the model of Gamermann and Oset [21,28] as described above.

In Ref. [28] it was found that the  $X(3872)$  had couplings to the charged and neutral components of  $DD^*$  that were very close to each other, implying an approximate  $I = 0$  character for the state. Since the masses and bindings used

<sup>3</sup>The formalism also makes approximations setting  $|\vec{q}|/M_V$  to zero, with  $\vec{q}$  the on-shell momentum of the vectors. Improvements on this were done in Ref. [23] (see Appendix B), which, when applied to the present problem, lead to negligible corrections.

TABLE I. Couplings  $g_R$  of the pole at  $(3871.6 - i0.001)$  MeV to the channels ( $\alpha_H = -1.27$  here).

Channel	$ g_{R \rightarrow PV} $ [MeV]
$(K^-K^{*+} - \text{c.c.})/\sqrt{2}$	–53
$(K^0\bar{K}^{*0} - \text{c.c.})/\sqrt{2}$	–49
$(D^-D^{*+} - \text{c.c.})/\sqrt{2}$	3638
$(D^0\bar{D}^{*0} - \text{c.c.})/\sqrt{2}$	3663
$(D_s^-D_s^{*+} - \text{c.c.})/\sqrt{2}$	3395

in Refs. [21,28] have been updated, we have redone the calculation of Gamermann and Oset [21,28] with updated masses, assuming the present binding of 0.2 MeV of the  $X(3872)$  with respect to the  $D^0\bar{D}^{*0} - \text{c.c}$  component. In Ref. [28] we have two subtraction constants,  $\alpha_L$  and  $\alpha_H$  (for the light and heavy sector) in the pseudoscalar-vector loop functions, and in view of the minor role played by the light channel, only the  $\alpha_H$  parameter was varied to fix the new binding of the  $X(3872)$ . The couplings to the channels are then reevaluated. They are obtained from the residues at the pole of the  $X(3872)$  resonance, which is obtained from a coupled channels unitary approach to the  $DD^* - \text{c.c}$ . interaction. This approach, an extension of the chiral unitary approach to the charm sector, accounts for the rescattering of the components and resums all the diagrams of the Bethe-Salpeter equation. The residue at the pole of the  $t_{ij}$  scattering matrix, where  $i$  and  $j$  are two channels, is given by  $g_i g_j$ , where  $g_i$  are the couplings. The results of the couplings are shown in Table I.

From the couplings in Table I, we observe that there is some isospin violation, which is however very small, less than 1%. Intuitively, one might think that the  $D^0\bar{D}^{*0}$  component is the only one relevant, because the binding of the  $D^0\bar{D}^{*0}$  is very small, of the order of 0.2 MeV and the wave function extends much further than for the charged component, which is bound by about 8 MeV. However, as we mentioned, the relevant interactions in most processes are short ranged and so the wave functions around the origin, proportional to the couplings in the approach we follow, are what matters.<sup>4</sup> Thus the wave function of the  $X(3872)$  is very close to the isospin  $I = 0$  combination of  $D^0\bar{D}^{*0} - \text{c.c}$ . and  $D^+D^{*-} - \text{c.c}$ . and has a sizable fraction of the  $D^+D^{*-} - \text{c.c}$ . of Eq. (1). However, in a field theoretical approach, like the one we follow, one only needs the couplings to calculate observables, without having to

<sup>4</sup>In Ref. [17], using a potential  $V(\vec{q}, \vec{q}') = v\Theta(\Lambda - \vec{q}) \times \Theta(\Lambda - \vec{q}')$ , one proves that  $gG = \Psi(\vec{r} = 0)$ , but with other regulators instead of the sharp cutoff,  $\Psi(\vec{r} = 0)$  is replaced by the function around the origin. Close to a pole, where  $1 - vG = 0$ , one can trade  $V$  and  $G$  changing  $\delta V = -\delta G$ , and the wave function at the origin would change. The freedom is reduced if one reproduces experimental data in a wider energy range and certainly for the ratio of couplings of two channels. For what concerns the present work, it suffices to keep in mind that the mentioned relationship provides a qualitative picture to distinguish wave functions and probabilities.

invoke the wave functions explicitly. The dynamics of the process in one reaction like ours, with propagators and couplings in the loops, determine the effective range of the process (see also Ref. [52] in this respect).

From Table I we can also see that the couplings to the  $K^- K^{*+} - \text{c.c.}$  and  $K^0 \bar{K}^{*0} - \text{c.c.}$  channels represent less than the 1% of the contributions from the other channels (the  $\pi^- \rho^+ - \text{c.c.}$  has even smaller strength). Therefore, we will treat the  $X(3872)$  as if it were dynamically generated only from the last three channels in the Table.

We have mentioned before that the Weinberg compositeness condition essentially provided the couplings of the  $X(3872)$  to the  $D^0 \bar{D}^{*0}$  component. We can see this now from a different perspective using the generalization of the Weinberg compositeness condition to coupled channels [17]. The sum rule obtained in Ref. [17] for dynamically generated states is

$$-\sum_i g_i^2 \frac{\partial G}{\partial s} = 1, \quad (4)$$

where  $g_i$  are the couplings of the state to any of the channels and  $G$  is the loop function of Eq. (3) regularized with a subtraction in Refs. [21,28], leading to

$$G = \frac{1}{16\pi^2} \left( \alpha_l + \log \frac{m_l^2}{\mu^2} + \frac{M_l^2 - m_l^2 + s}{2s} \log \frac{M_l^2}{m_l^2} + \frac{\tilde{p}}{\sqrt{s}} \left( \log \frac{s - M_l^2 + m_l^2 + 2\tilde{p}\sqrt{s}}{-s + M_l^2 - m_l^2 + 2\tilde{p}\sqrt{s}} + \log \frac{s + M_l^2 - m_l^2 + 2\tilde{p}\sqrt{s}}{-s - M_l^2 + m_l^2 + 2\tilde{p}\sqrt{s}} \right) \right), \quad (5)$$

where  $\tilde{p}$  is the 3-momentum in the center-of-mass reference frame and  $M_l$  and  $m_l$  are the two particles in the loop. The expression of  $G$  in Eq. (5) is commonly called the dimensional regularization formula [39]. The subtraction constants  $\alpha_l$ , of natural size [39], are finally tuned within

reasonable ranges to obtain the generated resonance at the right physical energy. In Ref. [28] one takes  $\alpha_L$  and  $\alpha_H$  for the light and heavy sectors. As mentioned above, in the present work we refitted the  $\alpha_H$  to the new binding of the  $X(3872)$ . Note that the subtraction constant in the regularization of Eq. (5) does not play a role in the derivative of  $G$  in Eq. (4), which is now convergent.

As shown in Ref. [17], each one of the terms in Eq. (4) stands for the probability of finding the  $i$  channel in the wave function, while  $gG$  measures the wave function at the origin. The numerical values obtained for the terms in Eq. (4) are 0.86 for  $D^0 \bar{D}^{*0}$ , 0.124 for  $D^+ D^{*-}$ , 0.016 for  $D_s^+ D_s^{*-}$ . As one can see, the probability of finding the  $D^0 \bar{D}^{*0}$  component is the largest, due to the small binding energy [35].

## B. The radiative decay $X(3872) \rightarrow J/\psi \gamma$

In the framework described above, the  $X(3872)$  decays into  $J/\psi \gamma$  through the diagrams shown in Fig. 1. From this figure we observe that there are four kinds of different Feynman diagrams, all of them with an anomalous vertex coupling two vectors and a pseudoscalar, depending on whether the diagram contains a PPV or a 3V vertex, or the photon emerges from the anomalous vertex. To begin with, there are three different channels:  $D^0 \bar{D}^{*0}$ ,  $D^+ D^{*-}$ , and  $D_s^+ D_s^{*-}$ , which lead to 12, plus another 12 for the complex conjugate Feynman diagrams to evaluate. The formalism used is very similar to the one of Molina *et al.* [53], where the authors study the radiative decay of the dynamically generated resonance  $K_2^*(1430)$  [54] into  $K \gamma$ , via diagrams containing anomalous vector-vector-pseudoscalar vertices. The VPP, 3V, and  $V\gamma$  vertices are evaluated using the local hidden gauge approach [24–27], which automatically incorporates vector meson dominance, by means of which the photons couple to other hadrons converting themselves into  $\rho^0$ ,  $\omega$ ,  $\phi$ , and  $J/\psi$ . As a consequence of this, we are

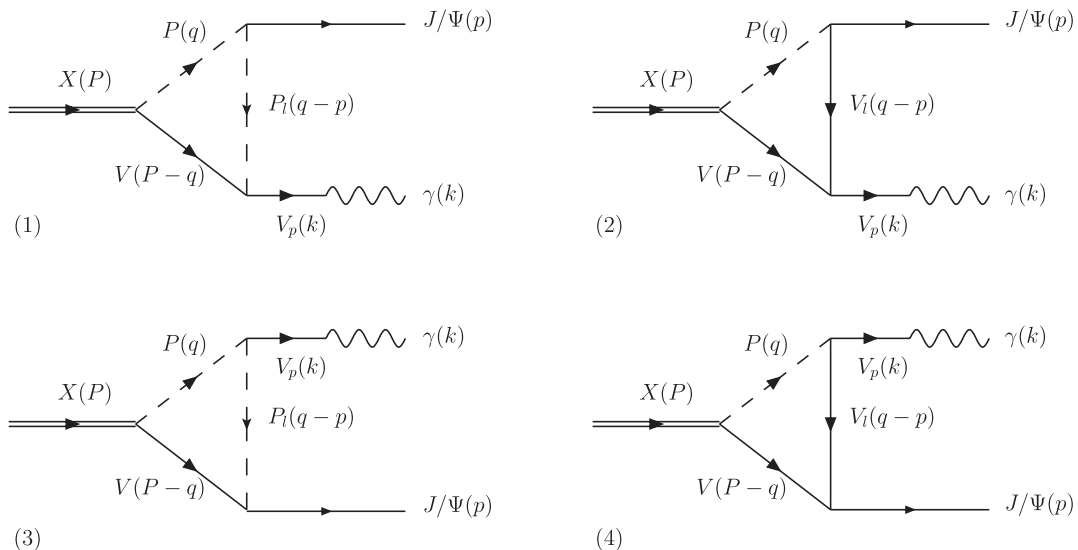


FIG. 1. Different types of Feynman diagrams for the decay of the  $X(3872)$  into  $J/\psi \gamma$ .

also able to evaluate the rates of the X(3872) decay into  $J/\psi\rho$ ,  $J/\psi\omega$  and the ratios of the decay rates, which can be compared to existing data.

In summary, the Lagrangians we need in order to evaluate the amplitudes are the following:

$$\mathcal{L}_{\text{VVP}} = \frac{G'}{\sqrt{2}} \epsilon^{\mu\nu\alpha\beta} \langle \partial_\mu V_\nu \partial_\alpha V_\beta P \rangle, \quad (6)$$

$$\mathcal{L}_{V\gamma} = -M_V^2 \frac{e}{g} A_\mu \langle V^\mu Q \rangle, \quad (7)$$

$$\mathcal{L}_{\text{PPV}} = -ig \langle V^\mu [P, \partial_\mu P] \rangle, \quad (8)$$

$$\mathcal{L}_{3V} = ig \langle (V^\mu \partial_\nu V_\mu - \partial_\nu V_\mu V^\mu) V^\nu \rangle, \quad (9)$$

with  $e$  the electron mass ( $e^2/4\pi = \alpha$ ),  $G' = 3g'^2/(4\pi^2 f)$ ,  $g' = -G_V M_\rho/(\sqrt{2}f^2)$ ,  $G_V = f/\sqrt{2}$ , and  $g = M_V/2f$ . The constant  $f$  is the pion decay constant  $f_\pi = 93$  MeV,  $Q = \text{diag}(2, -1, -1, 2)/3$ , and  $M_V$  is the mass of the vector meson, for which we take  $M_\rho$ .

The  $P$  and  $V$  matrices contain the 15-plet of the pseudoscalars and the 15-plet of vectors, respectively, in the physical basis considering  $\eta$ ,  $\eta'$  mixing [55],

$$P = \begin{pmatrix} \frac{\eta}{\sqrt{3}} + \frac{\eta'}{\sqrt{6}} + \frac{\pi^0}{\sqrt{2}} & \pi^+ & K^+ & \bar{D}^0 \\ \pi^- & \frac{\eta}{\sqrt{3}} + \frac{\eta'}{\sqrt{6}} - \frac{\pi^0}{\sqrt{2}} & K^0 & D^- \\ K^- & \bar{K}^0 & -\frac{\eta}{\sqrt{3}} + \sqrt{\frac{2}{3}}\eta' & D_s^- \\ D^0 & D^+ & D_s^+ & \eta_c \end{pmatrix}, \quad (10)$$

and  $V_\mu$  represents the vector nonet

$$V_\mu = \begin{pmatrix} \frac{\omega+\rho^0}{\sqrt{2}} & \rho^+ & K^{*+} & \bar{D}^{*0} \\ \rho^- & \frac{\omega-\rho^0}{\sqrt{2}} & K^{*0} & D^{*-} \\ K^{*-} & \bar{K}^{*0} & \phi & D_s^{*-} \\ D^{*0} & D^{*+} & D_s^{*+} & J/\psi \end{pmatrix}_\mu. \quad (11)$$

From Eqs. (6)–(9), we can write the vertices involved in the diagram of type (1) of Fig. 1 as

$$\begin{aligned} t_{RVP} &= g_X \epsilon^{(V)\mu} \epsilon_\mu^{(X)} & t_{V_p\gamma} &= PM_{V_p}^2 \frac{e}{g} \epsilon_\mu^{(y)} \epsilon^{(V_p)\mu} \\ t_{PPJ/\psi} &= P_V g (2q - p)_\mu \epsilon^{(J/\psi)\mu} & (12) \\ t_{VV_p P_1} &= AG' \epsilon^{\alpha\beta\gamma\delta} (P - q)_\alpha \epsilon_\beta^{(V)} k_\gamma \epsilon_\delta^{(V_1)}, \end{aligned}$$

where  $g_X = 3638/\sqrt{2}$ ,  $3663/\sqrt{2}$ ,  $3395/\sqrt{2}$  MeV, for  $D^- D^{*+}$ ,  $\bar{D}^0 D^{*0}$ ,  $D_s^- D_s^{*+}$  and  $-3638/\sqrt{2}$ ,  $-3663/\sqrt{2}$ ,  $-3395/\sqrt{2}$  MeV, for  $D^+ D^{*-}$ ,  $D^0 \bar{D}^{*0}$ ,  $D_s^+ D_s^{*-}$ , respectively, and  $P$ ,  $P_V$ , and  $A$  are numerical factors.

The  $V_p \rightarrow \gamma$  conversion essentially replaces, up to a constant,  $\epsilon_\delta^{(V_p)}$  with  $\epsilon_\delta^{(\gamma)}$ . Therefore, we can write the amplitude of the diagram (1) depicted in Fig. 1 as

$$\begin{aligned} -it_1 &= -B e g_X G' \int \frac{d^4 q}{(2\pi)^4} \epsilon^{(V)\beta'} \epsilon_{\beta'}^{(X)} \epsilon^{(J/\psi)\mu} \\ &\times (2q - p)_\mu \epsilon^{\alpha\beta\gamma\delta} (P - q)_\alpha \epsilon_\beta^{(V)} k_\gamma \epsilon_\delta^{(\gamma)} \frac{1}{q^2 - m_p^2} \\ &\times \frac{1}{(q - p)^2 - m_{P_1}^2} \frac{1}{(P - q)^2 - m_V^2}, \quad (13) \end{aligned}$$

where  $B = PAP_V$  (the values of  $B$  for each case are shown in Table II). Summing over the polarizations of the internal vector, we have

$$\sum_\lambda \epsilon_\beta^{(V)} \epsilon_{\beta'}^{(V)} = -g_{\beta\beta'} + \frac{(P - q)_\beta (P - q)_{\beta'}}{m_V^2}. \quad (14)$$

When contracting with the antisymmetric tensor  $\epsilon^{\alpha\beta\gamma\delta}$ , the term  $(P - q)_\beta (P - q)_{\beta'}$  disappears. Thus, we have an integral like

TABLE II. Coefficients  $B$  and  $C$  of the different diagrams in Fig. 1.

Diagram	P	V	$P_1$	B	
1	$D^0$	$\bar{D}^{*0}$	$D^0$	$\frac{4}{3\sqrt{2}}$	
	$D^+$	$D^{*-}$	$D^+$	$\frac{1}{3\sqrt{2}}$	
	$D_s^+$	$D_s^{*-}$	$D_s^+$	$\frac{1}{3\sqrt{2}}$	
	$\bar{1}$	$\bar{D}^0$	$D^{*0}$	$-\frac{4}{3\sqrt{2}}$	
1	$D^-$	$D^{*+}$	$D^-$	$-\frac{1}{3\sqrt{2}}$	
	$D_s^-$	$D_s^{*+}$	$D_s^-$	$-\frac{1}{3\sqrt{2}}$	
	3	$D^0$	$\bar{D}^{*0}$	0	
	$D^+$	$D^{*-}$	$D^+$	$\frac{1}{\sqrt{2}}$	
3	$D_s^+$	$D_s^{*-}$	$D_s^+$	$-\frac{1}{\sqrt{2}}$	
	$\bar{3}$	$\bar{D}^0$	$D^{*0}$	0	
	$D^-$	$D^{*+}$	$D^-$	$-\frac{1}{\sqrt{2}}$	
	$D_s^-$	$D_s^{*+}$	$D_s^-$	$-\frac{1}{\sqrt{2}}$	
Diagram	P	V	$V_1$	C	
2	$D^0$	$\bar{D}^{*0}$	$D^{*0}$	0	
	$D^+$	$D^{*-}$	$D^{*+}$	$-\frac{1}{\sqrt{2}}$	
	$D_s^-$	$D_s^{*+}$	$D_s^{*+}$	$\frac{1}{\sqrt{2}}$	
	$\bar{2}$	$\bar{D}^0$	$D^{*0}$	$\bar{D}^{*0}$	0
2	$D^-$	$D^{*+}$	$D^{*-}$	$\frac{1}{\sqrt{2}}$	
	$D_s^-$	$D_s^{*+}$	$D_s^{*-}$	$\frac{1}{\sqrt{2}}$	
	4	$D^0$	$\bar{D}^{*0}$	$D^{*0}$	$-\frac{4}{3\sqrt{2}}$
	$D^+$	$D^{*-}$	$D^{*+}$	$-\frac{1}{3\sqrt{2}}$	
4	$D_s^+$	$D_s^{*-}$	$D_s^{*+}$	$-\frac{1}{3\sqrt{2}}$	
	$\bar{4}$	$\bar{D}^0$	$D^{*0}$	$\bar{D}^{*0}$	$\frac{4}{3\sqrt{2}}$
	$D^-$	$D^{*+}$	$D^{*-}$	$\frac{1}{3\sqrt{2}}$	
	$D_s^-$	$D_s^{*+}$	$D_s^{*-}$	$\frac{1}{3\sqrt{2}}$	

$$\int \frac{d^4 q}{(2\pi)^4} \frac{(2q-p)_\mu (p+k-q)_\alpha}{(q^2 - m_p^2 + i\epsilon)((q-p)^2 - m_{p_l}^2 + i\epsilon)((p+k-q)^2 - m_V^2 + i\epsilon)} = i(ag_{\mu\alpha} + bk_\mu k_\alpha + cp_\alpha k_\mu + dk_\alpha p_\mu + ep_\alpha p_\mu) \quad (15)$$

because of Lorentz covariance. After contracting with the antisymmetric tensor  $\epsilon^{\alpha\beta\gamma\delta}$  and applying the Lorentz condition  $p_\mu \epsilon^{(J/\psi)\mu} = 0$ , only the coefficients  $a$  and  $c$  remain to be evaluated. The  $a$  coefficient is related to the logarithmically divergent part of the integral in Eq. (15) and, therefore, the evaluation of this coefficient needs special treatment as we will see later on. We arrive at an amplitude of the form

$$t_1 = BeG^l g_X \epsilon^{\alpha\beta\gamma\delta} (a \epsilon_\alpha^{(J/\psi)} + cp_\alpha k \cdot \epsilon^{(J/\psi)}) \epsilon_\beta^{(X)} k_\gamma \epsilon_\delta^{(\gamma)}. \quad (16)$$

Now we want to evaluate the  $a$  and  $c$  coefficients. We do it using the formula of the Feynman parametrization for  $n = 3$ ,

$$\frac{1}{\alpha\beta\gamma} = 2 \int_0^1 dx \int_0^x dy \frac{1}{[\alpha + (\beta - \alpha)x + (\gamma - \beta)y]^3}. \quad (17)$$

In the integral of Eq. (15), we can perform the above parametrization with

$$\begin{aligned} \alpha &= (q-p)^2 - m_{p_l}^2 & \beta &= q^2 - m_p^2 \\ \gamma &= (p+k-q)^2 - m_V^2. \end{aligned} \quad (18)$$

We define a new variable  $q' = q + p(x-y-1) - ky$ , such that the integral of Eq. (15) can be expressed as

$$4 \int_0^1 dx \int_0^x dy \int \frac{d^4 q'}{(2\pi)^4} \times \frac{(q' + p(1-x+y) + ky)_\mu (k - q' - p(y-x) - ky)_\alpha}{(q'^2 + s_1)^3}, \quad (19)$$

with

$$s_1 = -m_{p_l}^2 + (m_{p_l}^2 - m_p^2)x + (k^2 + m_p^2 - m_V^2)y + p^2(x-y)(1-x+y) + 2pky(x-y) - k^2y^2. \quad (20)$$

From Eq. (19), we must take the  $iag_{\mu\alpha}$  and  $icp_\alpha k_\mu$  terms. The  $c$  coefficient can be evaluated very easily, since

$$\int \frac{d^4 q'}{(q'^2 + s_1)^3} = \frac{i\pi^2}{2s_1}, \quad (21)$$

and we have

$$c = \frac{1}{8\pi^2} \int_0^1 dx \int_0^x dy \frac{y(x-y)}{s_1}. \quad (22)$$

The evaluation of the  $a$  coefficient is a little bit more elaborated. We have the identity

$$iag_{\mu\alpha} = -4 \int_0^1 dx \int_0^x dy \int \frac{d^4 q'}{(2\pi)^4} \frac{q'_\mu q'_\alpha}{(q'^2 + s_1 + i\epsilon)^3}, \quad (23)$$

and after taking the trace,

$$ia = - \int_0^1 dx \int_0^x dy \int \frac{d^4 q'}{(2\pi)^4} \frac{q'^2}{(q'^2 + s_1 + i\epsilon)^3}. \quad (24)$$

This part is logarithmically divergent and we will relate it to the two-meson function loop  $G(P)$  of Eq. (3) as follows: we multiply the integrand of Eq. (3) by the factor  $((q-p)^2 - m_{p_l}^2)/((q-p)^2 - m_{p_l}^2)$  and using the Feynman parametrization with the change of variable  $q' = q + p(x-y-1) - ky$ , we obtain

$$G(P) = 2i \int_0^1 dx \int_0^x dy \int \frac{d^4 q'}{(2\pi)^4} \times \frac{q'^2 + (ky)^2 + 2pky(y-x) + p^2(x-y)^2 - m_{p_l}^2}{(q' + s_1)^3} \quad (25)$$

and

$$a = \frac{G(P)}{2} + \frac{1}{32\pi^2} \int_0^1 dx \times \int_0^x dy \frac{(ky)^2 + 2pky(y-x) + p^2(x-y)^2 - m_{p_l}^2}{s_1 + i\epsilon}. \quad (26)$$

However, to assume that the divergent term of Eq. (24) in the three-particle loop can be regularized like in the two-body loop function appearing in scattering requires a justification. Certainly, this derivation only makes sense if there is a common cutoff in the two integrals. Indeed, the use of the same cutoff can be justified writing the potential of the chiral unitary approach as [17]

$$V(\vec{q}, \vec{q}', E) = v(E) \Theta(q_{\max} - |\vec{q}|) \Theta(q_{\max} - |\vec{q}'|), \quad (27)$$

which led to a  $T$  matrix with the same factorization

$$T(\vec{q}, \vec{q}', E) = T(E) \Theta(q_{\max} - |\vec{q}|) \Theta(q_{\max} - |\vec{q}'|). \quad (28)$$

This means that the  $PV \rightarrow PV$  amplitude in the  $X(3872)$  pole goes as

$$T \sim \frac{g_X \Theta(q_{\max} - |\vec{q}|) g_X \Theta(q_{\max} - |\vec{q}'|)}{s - M_X^2}, \quad (29)$$

and hence the cutoff of the scattering is inherent to the vertex in the  $X \rightarrow D\bar{D}^*$ , which is used in Fig. 1. The derivation above assumes that no extra cutoffs come from the other vertices in the diagrams, as usually assumed in most calculations, or that they involve bigger cutoffs which become then redundant. In order to test the accuracy of this procedure, we introduce an extra cutoff in the  $J/\psi DD^*$  vertex,  $\Theta(\Lambda' - |\vec{q}|)$ . For this we first evaluate the cutoff equivalent of the  $G$  function of scattering in dimensional regularization used in Refs. [21,28]. We find a cutoff of  $q_{\max} = 751.7$  MeV for the  $D^0\bar{D}^{*0}$  channel and  $q_{\max} = 733.3$  MeV for the  $D^+D^{*-}$  channel. We take  $q_{\max} = 700$  MeV for the  $D_S^+D_S^{*-}$  channel. Any larger value  $\Lambda'$  of the  $J/\psi DD^*$  cutoff,  $\Theta(\Lambda' - |\vec{q}|)$ , will not make any change. So we choose values of  $\Lambda'$  smaller than  $q_{\max}$  but in a reasonable range.

Another possibility is to take a form factor of the type  $e^{q^2/\Lambda'^2}$ . Such a form factor, with  $\Lambda' = 1.2$  MeV, was taken in Ref. [56] in a similar vertex involving  $D$  mesons, the  $D^*D\pi$  vertex. Normalized such that it is unity when we have the intermediate  $D\bar{D}^*$  on shell, the extra factor to be

$$-it_2 = -eG'g_X C \int \frac{d^4q}{(2\pi)^4} \epsilon^{\alpha\beta\gamma\delta} (q-p)_\alpha \epsilon_\beta^{(V_i)} p_\gamma \epsilon_\delta^{(J/\psi)} \epsilon_\nu^{(X)} \epsilon^{(V)\nu'} \{ (q-p+k)_\mu \epsilon_\nu^{(V_i)} \epsilon^{(V)\mu} \epsilon^{(\gamma)\nu} - (p+2k-q)_\nu \epsilon_\mu^{(V)} \epsilon^{(V_i)\nu} \epsilon^{(\gamma)\mu} + (2(p-q)+k)_\nu \epsilon_\mu^{(V)} \epsilon^{(\gamma)\nu} \epsilon^{(V_i)\mu} \} \frac{1}{q^2 - m_p^2 + i\epsilon} \frac{1}{(q-p)^2 - m_{V_i}^2 + i\epsilon} \times \frac{1}{(p+k-q)^2 - m_V^2 + i\epsilon},$$

where  $C = V_3PA$ . In this process the  $\bar{D}^{*0}$  is very close to being on-shell with zero three-momentum. To be consistent with the approach of Gamermann and Oset [28], which is neglecting the three-momentum compared to the mass of the vector meson,  $|\vec{q}|/m_V \approx 0$ ,  $\epsilon^{(V)0} \approx 0$ , we perform the sum over polarizations as

$$\sum_\lambda \epsilon^{(V)\mu} \epsilon^{(V)\nu'} \simeq \delta^{(\mu\nu')\text{spatial}} = \delta^{ij}. \quad (31)$$

$$\int \frac{d^4q}{(2\pi)^4} \frac{q_\alpha (q-p+k)_{\nu'}}{(q^2 - m_p^2 + i\epsilon)((q-p)^2 - m_{V_i}^2 + i\epsilon)((p+k-q)^2 - m_V^2 + i\epsilon)} = i(a_1 g_{\alpha\nu'} + b_1 k_\alpha k_{\nu'} + c_1 p_\alpha k_{\nu'} + d_1 p_{\nu'} k_\alpha + e_1 p_{\nu'} p_\alpha) \quad (32)$$

and

$$\int \frac{d^4q}{(2\pi)^4} \frac{q_\alpha 2(p-q)_\nu}{(q^2 - m_p^2 + i\epsilon)((q-p)^2 - m_{V_i}^2 + i\epsilon)((p+k-q)^2 - m_V^2 + i\epsilon)} = i(a_2 g_{\alpha\nu} + b_2 k_\alpha k_\nu + c_2 p_\alpha k_\nu + d_2 k_\alpha p_\nu + e_2 p_\alpha p_\nu). \quad (33)$$

One can see that only the coefficients proportional to  $a_1, b_1, d_1, a_2,$  and  $d_2$  survive. Thus, we finally get

$$t_2 = -CeG'g_X \epsilon^{\alpha\beta\gamma\delta} \{ (a_1 \epsilon_\alpha^{(X)} + (b_1 k^\mu + d_1 p^\mu) \epsilon_\mu^{(X)} k_\alpha) \epsilon_\beta^{(\gamma)} + (a_2 \epsilon_\alpha^{(\gamma)} + d_2 \epsilon_\mu^{(\gamma)} p^\mu k_\alpha) \epsilon_\beta^{(X)} \} p_\gamma \epsilon_\delta^{(J/\psi)}, \quad (34)$$

considered in three-dimensional integration of the loop function is  $e^{(\vec{q}_{on}^2 - \vec{q}^2)/\Lambda'^2}$ .

Then, we take the two options,  $\Lambda' \simeq 600$  MeV with a sharp cutoff and the exponential form factor, and we see how much the results change.

Now, we want to calculate the amplitude for the second diagram in Fig. 1 containing the three-vector vertex. The only difference with the previous diagram is the three-vector vertex. Thus, the amplitudes corresponding to the three-vector vertex and the anomalous vertex are, respectively,

$$t_{VV_i V_p} = V_3 g \{ (q-p+k)_\mu \epsilon_\nu^{(V_i)} \epsilon^{(V)\mu} \epsilon^{(V_p)\nu} - (p+2k-q)_\nu \epsilon_\mu^{(V)} \epsilon^{(V_i)\nu} \epsilon^{(V_p)\mu} + (2(p-q)+k)_\nu \epsilon_\mu^{(V)} \epsilon^{(V_i)\mu} \epsilon^{(V_p)\nu} \} \\ t_{V_i J/\psi P} = AG' \epsilon^{\alpha\beta\gamma\delta} (q-p)_\alpha \epsilon_\beta^{(V_i)} p_\gamma \epsilon_\delta^{(J/\psi)}, \quad (30)$$

where  $V_3$  and  $A$  are numerical factors.

Thus, we can write the amplitude of the diagram (2) in Fig. 1 as

We also can keep the covariant formalism and remember at the end that  $\mu, \nu'$  are spatial. The way to proceed is very similar to that of the previous diagram. The second term of the three-vector vertex proportional to  $(p+2k-q)_\beta$  does not contribute, since we have  $(q-p)_\alpha p_\gamma (p+2k-q)_\beta = q_\alpha (p+2k)_\beta p_\gamma \epsilon^{\alpha\beta\gamma\delta}$ , which applying Lorentz covariance in the integral turns into a term like  $(a' p_\alpha k_\beta + b' p_\beta k_\alpha) p_\gamma \epsilon^{\alpha\beta\gamma\delta} = 0$ . Therefore, we have two kinds of integrals,

where now

$$\begin{aligned}
 a_1 &= -\frac{G(P)}{4} - \frac{1}{64\pi^2} \int_0^1 dx \int_0^x dy \frac{(ky)^2 + 2pky(y-x) + p^2(x-y)^2 - m_{V_l}^2}{s_2 + i\epsilon} & b_1 &= \frac{1}{16\pi^2} \int_0^1 dx \int_0^x dy \frac{y(y+1)}{s_2 + i\epsilon} \\
 d_1 &= \frac{1}{16\pi^2} \int_0^1 dx \int_0^x dy \frac{y(y-x)}{s_2 + i\epsilon} & a_2 &= -2a_1 & d_2 &= -2d_1,
 \end{aligned} \quad (35)$$

with

$$s_2 = -m_{V_l}^2 + (m_{V_l}^2 - m_P^2)x + (k^2 - m_V^2 + m_P^2)y + p^2(x-y)(1-x+y) + 2kyp(x-y) - k^2y^2. \quad (36)$$

In order to evaluate diagrams (3) and (4) in Fig. 1, we only have to do the exchanges  $k \leftrightarrow p$  and  $\epsilon^{(\gamma)} \leftrightarrow \epsilon^{(J/\psi)}$  in the amplitudes of diagrams (1) and (2).

We have

$$t_3 = BeG'g_X^c \epsilon^{\alpha\beta\gamma\delta} (a\epsilon_\alpha^{(\gamma)} + dk_\alpha(p \cdot \epsilon^{(\gamma)})) \epsilon_\beta^{(X)} p_\gamma \epsilon_\delta^{(J/\psi)}, \quad (37)$$

with

$$\begin{aligned}
 a &= \frac{G(P)}{2} + \frac{1}{32\pi^2} \int_0^1 dx \\
 &\times \int_0^x dy \frac{(py)^2 + 2pky(y-x) - m_{P_l}^2}{s_3 + i\epsilon}, \quad (38)
 \end{aligned}$$

and

$$d = \frac{1}{8\pi^2} \int_0^1 dx \int_0^x dy \frac{y(x-y)}{s_3}, \quad (39)$$

where

$$s_3 = -m_{P_l}^2 + (m_{P_l}^2 - m_P^2)x + (p^2 + m_P^2 - m_V^2)y + 2pky(x-y) - p^2y^2, \quad (40)$$

for diagram (3), and

$$\begin{aligned}
 t_4 &= -CeG'g_X \epsilon^{\alpha\beta\gamma\delta} \{ (a_1\epsilon_\alpha^{(X)} \\
 &+ (c_1k^\mu + e_1p^\mu)\epsilon_\mu^{(X)} p_\alpha\epsilon_\beta^{(J/\psi)} \\
 &+ (a_2\epsilon_\alpha^{(J/\psi)} + c_2\epsilon_\mu^{(J/\psi)} k^\mu p_\alpha)\epsilon_\beta^{(X)} \} k_\gamma \epsilon_\delta^{(\gamma)}, \quad (41)
 \end{aligned}$$

with

$$\begin{aligned}
 a_1 &= -\frac{G(p)}{4} - \frac{1}{64\pi^2} \int_0^1 dx \\
 &\times \int_0^x dy \frac{(py)^2 + 2pky(y-x) - m_{V_l}^2}{s_4 + i\epsilon} \\
 e_1 &= \frac{1}{16\pi^2} \int_0^1 dx \int_0^x dy \frac{y(y+1)}{s_4 + i\epsilon} \\
 c_1 &= \frac{1}{16\pi^2} \int_0^1 dx \int_0^x dy \frac{y(y-x)}{s_4 + i\epsilon} \\
 a_2 &= -2a_1 & c_2 &= -2c_1, \quad (42)
 \end{aligned}$$

and

$$s_4 = -m_{V_l}^2 + (m_{V_l}^2 - m_P^2)x + (p^2 - m_V^2 + m_P^2)y + 2kyp(x-y) - p^2y^2 \quad (43)$$

for diagram (4).

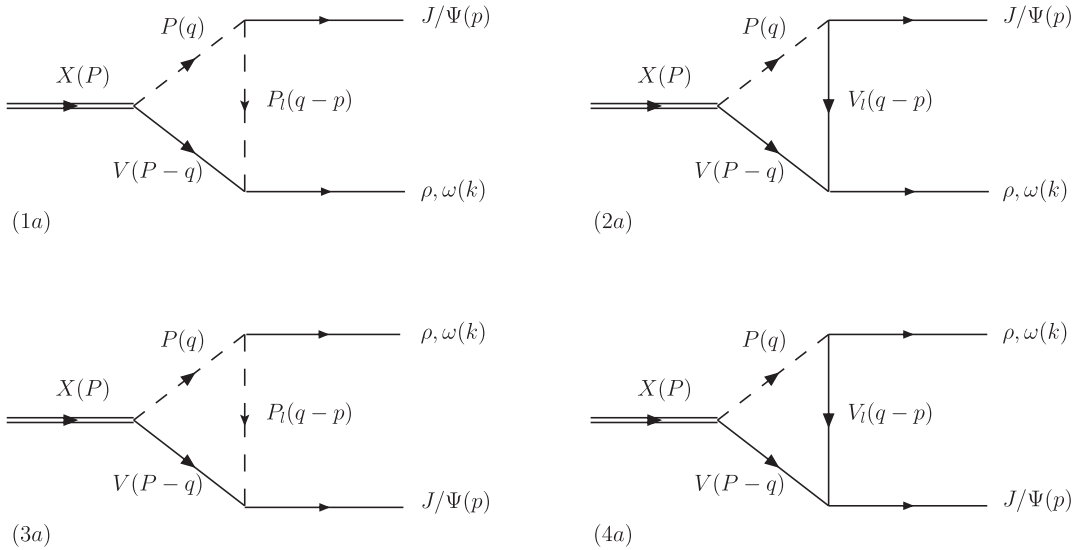


FIG. 2. Different types of Feynman diagrams for the decay of the  $X(3872)$  into  $J/\psi\rho$  and  $J/\psi\omega$ .

TABLE III. Coefficients  $B'$  and  $C'$  of the different diagrams in Fig. 2 in the case of a  $\rho$  meson in the final state.

Diagram	P	V	$P_1$	$B'$
1	$D^0$	$\bar{D}^{*0}$	$D^0$	$\frac{1}{2}$
	$D^+$	$D^{*-}$	$D^+$	$-\frac{1}{2}$
$\bar{1}$	$\bar{D}^0$	$D^{*0}$	$\bar{D}^0$	$-\frac{1}{2}$
	$D^-$	$D^{*+}$	$D^-$	$-\frac{1}{2}$
3	$D^0$	$\bar{D}^{*0}$	$D^0$	$-\frac{1}{2}$
	$D^+$	$D^{*-}$	$D^+$	$\frac{1}{2}$
$\bar{3}$	$\bar{D}^0$	$D^{*0}$	$\bar{D}^0$	$\frac{1}{2}$
	$D^-$	$D^{*+}$	$D^-$	$-\frac{1}{2}$

---

Diagram	P	V	$V_1$	$C'$
2	$D^0$	$\bar{D}^{*0}$	$D^{*0}$	$\frac{1}{2}$
	$D^+$	$D^{*-}$	$D^{*+}$	$-\frac{1}{2}$
$\bar{2}$	$\bar{D}^0$	$D^{*0}$	$\bar{D}^{*0}$	$-\frac{1}{2}$
	$D^-$	$D^{*+}$	$D^{*-}$	$\frac{1}{2}$
4	$D^0$	$\bar{D}^{*0}$	$D^{*0}$	$\frac{1}{2}$
	$D^+$	$D^{*-}$	$D^{*+}$	$-\frac{1}{2}$
$\bar{4}$	$\bar{D}^0$	$D^{*0}$	$\bar{D}^{*0}$	$-\frac{1}{2}$
	$D^-$	$D^{*+}$	$D^{*-}$	$\frac{1}{2}$

### C. The $X(3872)$ decay to $J/\psi \rho$ and $J/\psi \omega$

This formalism also allows us to evaluate the amplitudes for the decays  $X \rightarrow J/\psi \rho$  and  $X \rightarrow J/\psi \omega$  (Fig. 2). We can proceed in complete analogy with the radiative decay to determine these amplitudes, simply removing the final photon and leaving the vector meson in the final state, the  $\rho^0$  or the  $\omega$ . Moreover, we must take into account that the  $\rho^0$  and the  $\omega$  do not couple to the strange  $D$  mesons, so that we have again four different kinds of diagrams, but only two channels plus their complex conjugate, that is 16 Feynman diagrams to evaluate. Doing this, we can observe that the new amplitudes have the same structure as the previous ones and can be obtained, up to a coefficient, directly with the substitutions  $e \leftrightarrow g$  and  $\epsilon^{(\gamma)} \leftrightarrow \epsilon^{(\rho,\omega)}$ . For instance, in the case of the diagram (1a) of Fig. 2, we have

$$t_{1a} = B' g G' g_X \epsilon^{\alpha\beta\gamma\delta} (a \epsilon_\alpha^{(J/\psi)} + c p_\alpha k \cdot \epsilon^{(J/\psi)}) \epsilon_\beta^{(X)} k_\gamma \epsilon_\delta^{(\rho,\omega)}, \quad (44)$$

with  $a$  and  $c$  the same as before

$$a = \frac{G(P)}{2} + \frac{1}{32\pi^2} \int_0^1 dx \times \int_0^x dy \frac{(ky)^2 + 2pk_y(y-x) + p^2(x-y)^2 - m_{P_1}^2}{s_1 + i\epsilon},$$

$$c = \frac{1}{8\pi^2} \int_0^1 dx \int_0^x dy \frac{y(x-y)}{s_1} \quad (45)$$

TABLE IV. Coefficients  $B'$  and  $C'$  of the different diagrams in Fig. 2 in the case of a  $\omega$  meson in the final state.

Diagram	P	V	$P_1$	$B'$
1	$D^0$	$\bar{D}^{*0}$	$D^0$	$\frac{1}{2}$
	$D^+$	$D^{*-}$	$D^+$	$\frac{1}{2}$
$\bar{1}$	$\bar{D}^0$	$D^{*0}$	$\bar{D}^0$	$-\frac{1}{2}$
	$D^-$	$D^{*+}$	$D^-$	$-\frac{1}{2}$
3	$D^0$	$\bar{D}^{*0}$	$D^0$	$-\frac{1}{2}$
	$D^+$	$D^{*-}$	$D^+$	$-\frac{1}{2}$
$\bar{3}$	$\bar{D}^0$	$D^{*0}$	$\bar{D}^0$	$\frac{1}{2}$
	$D^-$	$D^{*+}$	$D^-$	$\frac{1}{2}$

---

Diagram	P	V	$V_1$	$C'$
2	$D^0$	$\bar{D}^{*0}$	$D^{*0}$	$\frac{1}{2}$
	$D^+$	$D^{*-}$	$D^{*+}$	$\frac{1}{2}$
$\bar{2}$	$\bar{D}^0$	$D^{*0}$	$\bar{D}^{*0}$	$-\frac{1}{2}$
	$D^-$	$D^{*+}$	$D^{*-}$	$-\frac{1}{2}$
4	$D^0$	$\bar{D}^{*0}$	$D^{*0}$	$\frac{1}{2}$
	$D^+$	$D^{*-}$	$D^{*+}$	$\frac{1}{2}$
$\bar{4}$	$\bar{D}^0$	$D^{*0}$	$\bar{D}^{*0}$	$-\frac{1}{2}$
	$D^-$	$D^{*+}$	$D^{*-}$	$-\frac{1}{2}$

and  $B' = P_V A$  of Eqs. (12). However, since we are dealing with different vertices, the new numerical coefficients, that we call  $B'$  and  $C'$ , are now different and they are written in Tables III and IV.

### III. RESULTS

Following the procedure in Sec. II, we can obtain the total decay amplitude for the radiative decay of the  $X$  meson and evaluate the correspondent decay width for this channel by means of the formula

$$\Gamma = \frac{|\vec{k}|}{8\pi M_X^2} \bar{\sum} \sum |t|^2, \quad (46)$$

where we sum over the polarizations of the final states and average over the  $X$  meson polarizations.

Applying Eq. (46), we obtain

$$\Gamma(X \rightarrow J/\psi \gamma) = 149.5 \text{ keV}. \quad (47)$$

In order to make an estimation of the theoretical uncertainty on this quantity, we perform a suitable variation of the parameters used to compute the total amplitude: the coupling  $G'$  for the vertex coupling two vectors and a pseudoscalar vertex [Eq. (6)], the axial-vector-pseudoscalar couplings  $g_X$  for the three channels, and the two subtraction constants in the loop function,  $\alpha$  and  $\alpha_S$ .

We allow the constant  $f$ , contained in  $G'$ , to vary, but keep the relationship  $G_V = f/\sqrt{2}$  and replace  $M_V = M_\rho$

with  $M_{D^*}$ . The couplings  $g_X$  for the neutral and strange channels are also varied, independently, by 10%. This might be extreme for the neutral channel, since it is basically determined by the Weinberg compositeness condition, but we also have an uncertainty in the binding which can induce this change. For that reason we perform later on another sort of error analysis based on experimental uncertainties. On the other hand, the variation of the coupling for the charged channel is done in such a way that the ratio between it and the one for the neutral channel is kept constant, in order to preserve the isospin of the  $X(3872)$ . Then, we let the subtraction constants  $\alpha$  and  $\alpha_S$  vary between  $-1.60$  and  $-1.27$ . This range is motivated by the range chosen for  $f$ . Indeed, going to higher values of the constant  $f$  causes a decrease of the potential in the Lippman-Schwinger equation used to evaluate the scattering amplitude which determines the position of the resonance. One would need to go to more negative values of the subtraction constants  $\alpha$  and  $\alpha_S$  in the loop function, which appears in the  $a$  coefficients, to keep the pole representing the resonance in the same position. The range is thus chosen such as to produce an effect in the pole position similar to that induced by the change in  $f$ .

We obtain the result

$$\Gamma(X \rightarrow J/\psi \gamma) = (117 \pm 40) \text{ keV}. \quad (48)$$

There is another source of error that stems from experimental uncertainties in the binding of the  $X(3872)$ , and we also evaluate it. We have then performed a different exercise changing just  $\alpha_H$  such that the binding goes from 0.1 to 0.4 MeV, which is indeed within the experimental limits but still keeps the  $X(3872)$  bound. We recalculate the couplings and evaluate again the rates and we find

$$\Gamma(X \rightarrow J/\psi \gamma) = (117^{+48}_{-35}) \text{ keV}. \quad (49)$$

This gives a new perspective on the uncertainties, showing that errors from the experimental uncertainties are of the same order of the rough estimate of the theoretical errors.

We can also evaluate the branching ratios for the decays  $X \rightarrow J/\psi \rho$  and  $X \rightarrow J/\psi \omega$ . These two decays, if we consider the  $\rho$  and the  $\omega$  with fixed masses, are not allowed because of the phase space, but they can occur when their mass distributions are taken into account and they are observed in the decays  $X \rightarrow J/\psi \pi \pi$  and  $X \rightarrow J/\psi \pi \pi \pi$ , respectively. The two- and three-pion states are produced in the decays of the  $\rho$  and the  $\omega$ .

Thus, the decay widths, convoluted with the spectral functions, are given by the formula

$$\begin{aligned} \Gamma_{\rho/\omega} &= \frac{1}{N} \int_{(m_{\rho/\omega}-2\Gamma_{\rho/\omega})^2}^{(m_{\rho/\omega}+2\Gamma_{\rho/\omega})^2} d\tilde{m}^2 \left( -\frac{1}{\pi} \right) \\ &\times \text{Im} \left[ \frac{1}{\tilde{m}^2 - m_{\rho/\omega}^2 + i\tilde{\Gamma}_{\rho/\omega}\tilde{m}} \right] \\ &\times \Gamma_X(\tilde{m}) \theta(m_X - m_{J/\psi} - \tilde{m}), \end{aligned} \quad (50)$$

where

$$N = \int_{(m_{\rho/\omega}-2\Gamma_{\rho/\omega})^2}^{(m_{\rho/\omega}+2\Gamma_{\rho/\omega})^2} d\tilde{m}^2 \left( -\frac{1}{\pi} \right) \text{Im} \left[ \frac{1}{\tilde{m}^2 - m_{\rho/\omega}^2 + i\tilde{\Gamma}_{\rho/\omega}\tilde{m}} \right], \quad (51)$$

where  $\Gamma_X(\tilde{m})$  is given by Eq. (46), replacing  $m_\rho$  and  $m_\omega$  with  $\tilde{m}$ .

In Eqs. (50) and (51),  $m_\rho = 775.49$  MeV and  $m_\omega = 782.65$  MeV are the masses of the mesons,  $\Gamma_\rho = 149.1$  MeV and  $\Gamma_\omega = 8.49$  MeV are the on-shell widths and

$$\tilde{\Gamma}_{\rho/\omega} = \Gamma_{\rho/\omega} \left( \frac{\tilde{q}}{q_{\rho/\omega}} \right)^3, \quad (52)$$

where  $\tilde{q}$  and  $q_{\rho/\omega}$  are the on-shell relative momenta of the mesons in the center-of-mass reference frame for the mass  $\tilde{m}$  and the physical mass, respectively,

$$\begin{aligned} \tilde{q} &= \frac{\sqrt{\tilde{m}^2 - 4m_\pi^2}}{2} \theta(\tilde{m} - 2m_\pi), \\ q_{\rho/\omega} &= \frac{\sqrt{m_{\rho/\omega}^2 - 4m_\pi^2}}{2}. \end{aligned} \quad (53)$$

In Eq. (50),  $\Gamma_X$  is the total decay width of the  $X$  into  $J/\psi \rho$  or  $J/\psi \omega$  to simplify the notation, and in Eq. (53),  $m_\pi$  is the pion mass.

Using Eq. (50) we find

$$\Gamma_\rho = 821.9 \text{ keV}, \quad \Gamma_\omega = 1096.6 \text{ keV}, \quad (54)$$

and when the error analysis that leads to Eq. (48) is done, the band of values becomes

$$\Gamma_\rho = (645 \pm 221) \text{ keV}, \quad \Gamma_\omega = (861 \pm 294) \text{ keV}. \quad (55)$$

Similarly to Eq. (49) we also have errors due to the uncertainties in the binding. Taking the same range that led to Eq. (48), we find

$$\Gamma_\rho = (645^{+264}_{-192}) \text{ keV}, \quad \Gamma_\omega = (861^{+353}_{-257}) \text{ keV}. \quad (56)$$

With the results of Eq. (54) we can evaluate the ratio

$$R = \frac{\mathcal{B}(X \rightarrow J/\psi \pi \pi \pi)}{\mathcal{B}(X \rightarrow J/\psi \pi \pi)} = \frac{\Gamma_\omega}{\Gamma_\rho} = 1.33. \quad (57)$$

However, the experiment gives the ratio [57]

$$R^{\text{exp}} = \frac{\mathcal{B}(X \rightarrow J/\psi \pi^+ \pi^- \pi^0)}{\mathcal{B}(X \rightarrow J/\psi \pi^+ \pi^-)} = 0.8 \pm 0.3 \quad (58)$$

and, to compare our result with this, we must take into account that the  $\omega$  decays into  $\pi^+ \pi^- \pi^0$  with a branching ratio  $B_{\omega,3\pi} = 0.892$ .

TABLE V. Values of the partial decay width in units of keV. First column: using the standard  $G$  function of scattering. Second column: multiplying the integrand of  $G$  by  $\theta(\Lambda' - |\vec{q}|)$  with  $\Lambda' = 600$  MeV. Third column: multiplying the integrand of  $G$  by  $e^{(\vec{q}_{on}^2 - \vec{q}^2)/\Lambda'^2}$  with  $\Lambda' = 1200$  MeV. Fourth column: range of values for all the rates including the three sources of errors, from uncertainties in the couplings, binding of the  $X$  and the  $G$  function, summed in quadrature. Fifth column: experimental results.

	Standard $G$	$\Theta(\Lambda' -  \vec{q} )$	$e^{(\vec{q}_{on}^2 - \vec{q}^2)/\Lambda'^2}$	Range	Experiment
$\Gamma_\gamma$	150	190	180	$117_{-53}^{+73}$	
$\Gamma_{\rho(2\pi)}$	821	991	905	$645_{-293}^{+383}$	
$\Gamma_{\omega(3\pi)}$	1097	1593	1380	$861_{-390}^{+500}$	
$\frac{\Gamma_\omega}{\Gamma_\rho} \times B_{\omega,3\pi}$	1.19	1.43	1.36	$0.92_{-0.13}^{+0.27}$	$0.8 \pm 0.3$ [57]
$\Gamma_\gamma/\Gamma_{\rho(2\pi)}$	0.18	0.19	0.20	$0.17_{-0.02}^{+0.03}$	$(0.14 \pm 0.05)$ [1] $(0.22 \pm 0.06)$ [2]

Hence, our ratio to compare with  $R^{\text{exp}}$  is

$$R^{\text{th}} = \frac{\Gamma_\omega}{\Gamma_\rho} \times B_{\omega,3\pi} = 1.19, \quad (59)$$

well within the experimental error.

The result we obtain for the ratio

$$\frac{\Gamma(X \rightarrow J/\psi \gamma)}{\Gamma(X \rightarrow J/\psi \pi \pi)} = 0.18, \quad (60)$$

is also compatible with the two values known from the experiment  $(0.14 \pm 0.05)$  [1] and  $(0.22 \pm 0.06)$  [2].

We can also estimate the theoretical errors for the two ratios in Eqs. (59) and (60), by evaluating the  $\gamma$ ,  $\rho$ , and  $\omega$  decays with the same set of parameters and varying these parameters in the range used to evaluate  $\Gamma(X \rightarrow J/\psi \gamma)$ ,

$$R^{\text{th}} = (0.92 \pm 0.13) \quad (61)$$

$$\frac{\Gamma(X \rightarrow J/\psi \gamma)}{\Gamma(X \rightarrow J/\psi \pi \pi)} = (0.17 \pm 0.02).$$

We should note that changing the binding, as done to get the errors in Eq. (49), barely changes the ratios of Eq. (61) since the ratios of the couplings of the  $X(3872)$  to the different channels barely change. This was already found in Ref. [28]. The uncertainties in the ratios are smaller than for the absolute values and they are of the order of 15%.

At this point we also take into account uncertainties from the association of the loop with two propagators to the  $G$  function of scattering, including extra cutoffs or the form factor discussed above. The values that we find are shown in Table V, where the errors from the three sources discussed are added in quadrature. We can see that we have good agreement with the experiment in the two ratios measured.

Finally, we do another exercise removing the  $D^+ D^{*-} - \text{c.c}$  and  $D_S^+ D_S^{*-} - \text{c.c}$  and allowing only the  $D^0 \bar{D}^{*0} - \text{c.c}$  contribution. The coupling of the  $D^0 \bar{D}^{*0} - \text{c.c}$  is reevaluated, taking the same binding for the  $X(3872)$ , such that Eq. (4) is now fulfilled with just this channel. The results that we obtain are

$$\Gamma_\gamma = 0.53 \text{ keV} \quad \Gamma_\rho = 10589 \text{ keV} \quad \Gamma_\omega = 429 \text{ keV}$$

$$R^{\text{th}} = 0.04 \quad \frac{\Gamma(X \rightarrow J/\psi \gamma)}{\Gamma(X \rightarrow J/\psi \pi \pi)} = 5.05 \cdot 10^{-5}. \quad (62)$$

As we can see, the two ratios that we have to compare with the experiment largely diverge from the experimental values, and  $\Gamma_\rho$  by itself becomes much bigger than the width of the  $X(3872)$  ( $\Gamma_X < 1.2$  MeV).

In Table VI we compare our results with a variety of results available in the literature using different models. It would be interesting to test these models with the new information on the experimental ratios to help discriminate among them.

The ratio of  $J/\psi \gamma$  to  $J/\psi \pi \pi$  is also evaluated in Ref. [9], where the Weinberg compositeness condition [15] is used to determine the couplings but other assumptions are made, and they find a range of values from 0.18 to 1.57, depending on the model they consider, as mentioned in the Introduction. We should stress that once the  $X$  is obtained in our case and, hence, the couplings are determined, the uncertainties that we have from theoretical sources and experimental errors in the masses are much smaller than in Ref. [9].

We should note that our results are tied to the masses of the particles in the PDG, and there are still large errors. When in the future the binding can be more accurately determined, we can also obtain more accurate values of the

TABLE VI. Results from previous works for the decay width of the  $X(3872)$  into  $J/\psi \gamma$ , using different models.

Model	$\Gamma$ [keV]
$c\bar{c}$	11 [5]
$c\bar{c}$	139 [6]
Molecule	8 [6]
Molecule	125–250 [8]
$c\bar{c}$	11–71 [9]
Molecule + $c\bar{c}$	2–17 [9]
$2^{--}$	1.7–2.1 [30]
$c\bar{c}$	45–80 [10]
Tetraquark	10–20 [11]
Present work	64–190

absolute rates. On the other hand, the values of the ratios will be essentially unaltered.

#### IV. CONCLUSIONS

In this paper we have exploited the picture of the  $X(3872)$  as a composite state of  $D\bar{D}^* - \text{c.c.}$  dynamically generated by the interaction of the  $D$  and  $D^*$  states. The couplings of the state to the different  $D\bar{D}^* - \text{c.c.}$  channels have been calculated before within this model, but we have recalculated them here to take into account the more precise values of the particle masses tabulated in the PDG [58]. The coupling for the  $D^0\bar{D}^{*0} - \text{c.c.}$  is similar to the one that would be obtained using the compositeness condition of Weinberg, since the state is barely bound in the  $D^0\bar{D}^{*0}$  component, but the dynamics of the model also produce couplings for the  $D^+D^{*-} - \text{c.c.}$  and  $D_S^+D_S^{*-} - \text{c.c.}$  states. Using an extension to  $SU(4)$  with an explicit breaking of this symmetry of the local hidden gauge approach, used before successfully in the study of related processes, one can determine the widths of the  $X(3872)$  to  $J/\psi\rho$ ,  $J/\psi\omega$ , and  $J/\psi\gamma$  and compare with the ratios determined experimentally in recent works. We find a very good agreement with the experimental results. The absolute numbers obtained for the different widths are also reasonable and their sum within errors,  $(1.6_{-0.7}^{+0.9})$  MeV, is compatible with the recent total  $X(3972)$  upper limit of the width,  $\Gamma = 1.2$  MeV.

We have also conducted a test neglecting the charged and strange components of the wave function, thus having only the  $D^0\bar{D}^{*0} - \text{c.c.}$  component. We obtain ratios in great disagreement with the experiment and an absolute value for the  $X(3872)$  partial width into  $J/\psi\rho$  that largely exceeds the experimental upper bound for the total width of the  $X(3872)$ . This exercise confirms the relevance of the charged channels to describe the process that we studied and the approximate  $I = 0$  character of this resonance. This does not mean that the use of the neutral channel alone is an incorrect way to proceed in general. It is just incomplete, but in any field theoretical approach, the missing channels can be accounted for by means of counterterms, which, however, make the theory less predictive. For the present case it became clear that the explicitly considering the charged  $D\bar{D}^*$  channels rendered the theory more predictive than omitting them.

#### ACKNOWLEDGMENTS

We would like to thank Dian-Yong Chen for useful information. This work is partly supported by the DGICYT Contract No. FIS2011-28853-C02-01, FEDER funds from the European Union, the Generalitat Valenciana in the program Prometeo, 2009/090, and the EU Integrated Infrastructure Initiative Hadron Physics 3 Project under Grant Agreement No. 283286.

- 
- [1] K. Abe *et al.* (Belle Collaboration), [arXiv:hep-ex/0505037](#).
  - [2] B. Aubert *et al.* (BABAR Collaboration), [Phys. Rev. D \*\*74\*\*, 071101 \(2006\)](#).
  - [3] V. Bhardwaj *et al.* (Belle Collaboration), [Phys. Rev. Lett. \*\*107\*\*, 091803 \(2011\)](#).
  - [4] T. Barnes and S. Godfrey, [Phys. Rev. D \*\*69\*\*, 054008 \(2004\)](#).
  - [5] E. Braaten and M. Kusunoki, [Phys. Rev. D \*\*69\*\*, 074005 \(2004\)](#).
  - [6] E. S. Swanson, [Phys. Lett. B \*\*598\*\*, 197 \(2004\)](#).
  - [7] E. Braaten and M. Kusunoki, [Phys. Rev. D \*\*72\*\*, 054022 \(2005\)](#).
  - [8] Y.-b. Dong, A. Faessler, T. Gutsche, and V.E. Lyubovitskij, [Phys. Rev. D \*\*77\*\*, 094013 \(2008\)](#).
  - [9] Y. Dong, A. Faessler, T. Gutsche, and V.E. Lyubovitskij, [J. Phys. G \*\*38\*\*, 015001 \(2011\)](#).
  - [10] A.M. Badalian, V.D. Orlovsky, Y.A. Simonov, and B.L.G. Bakker, [Phys. Rev. D \*\*85\*\*, 114002 \(2012\)](#).
  - [11] S. Dubnicka, A.Z. Dubnickova, M.A. Ivanov, J.G. Koerner, P. Santorelli, and G.G. Saidullaeva, [Phys. Rev. D \*\*84\*\*, 014006 \(2011\)](#).
  - [12] M. Nielsen and C.M. Zanetti, [Phys. Rev. D \*\*82\*\*, 116002 \(2010\)](#).
  - [13] R. D'Elia Matheus, F.S. Navarra, M. Nielsen, and C.M. Zanetti, [Phys. Rev. D \*\*80\*\*, 056002 \(2009\)](#).
  - [14] E. Braaten and M. Lu, [Phys. Rev. D \*\*77\*\*, 014029 \(2008\)](#).
  - [15] S. Weinberg, [Phys. Rev. \*\*130\*\*, 776 \(1963\)](#); S. Weinberg, [Phys. Rev. \*\*137\*\*, B672 \(1965\)](#).
  - [16] V. Baru, J. Haidenbauer, C. Hanhart, Y. Kalashnikova, and A.E. Kudryavtsev, [Phys. Lett. B \*\*586\*\*, 53 \(2004\)](#).
  - [17] D. Gamermann, J. Nieves, E. Oset, and E.R. Arriola, [Phys. Rev. D \*\*81\*\*, 014029 \(2010\)](#).
  - [18] A. Faessler, T. Gutsche, V.E. Lyubovitskij and Y.-L. Ma, [Phys. Rev. D \*\*76\*\*, 014005 \(2007\)](#).
  - [19] T. Branz, T. Gutsche, and V.E. Lyubovitskij, [Phys. Rev. D \*\*79\*\*, 014035 \(2009\)](#).
  - [20] Y. Dong, A. Faessler, T. Gutsche, S. Kovalenko, and V.E. Lyubovitskij, [Phys. Rev. D \*\*79\*\*, 094013 \(2009\)](#).
  - [21] D. Gamermann and E. Oset, [Eur. Phys. J. A \*\*33\*\*, 119 \(2007\)](#).
  - [22] C. Hidalgo-Duque, J. Nieves, and M.P. Valderrama, [arXiv:1210.5431](#).
  - [23] L. Roca, E. Oset, and J. Singh, [Phys. Rev. D \*\*72\*\*, 014002 \(2005\)](#).
  - [24] M. Bando, T. Kugo, S. Uehara, K. Yamawaki, and T. Yanagida, [Phys. Rev. Lett. \*\*54\*\*, 1215 \(1985\)](#).
  - [25] M. Bando, T. Kugo, and K. Yamawaki, [Phys. Rep. \*\*164\*\*, 217 \(1988\)](#).
  - [26] M. Harada and K. Yamawaki, [Phys. Rep. \*\*381\*\*, 1 \(2003\)](#).
  - [27] U.G. Meissner, [Phys. Rep. \*\*161\*\*, 213 \(1988\)](#).
  - [28] D. Gamermann and E. Oset, [Phys. Rev. D \*\*80\*\*, 014003 \(2009\)](#).

- [29] D. L. Canham, H.-W. Hammer, and R. P. Springer, *Phys. Rev. D* **80**, 014009 (2009).
- [30] M. Harada and Y.-L. Ma, *Prog. Theor. Phys.* **126**, 91 (2011).
- [31] C. Hanhart, Y. S. Kalashnikova, A. E. Kudryavtsev, and A. V. Nefediev, *Phys. Rev. D* **85**, 011501 (2012).
- [32] H.-W. Ke and X.-Q. Li, *Phys. Rev. D* **84**, 114026 (2011).
- [33] D. Gamermann and E. Oset, *Eur. Phys. J. A* **36**, 189 (2008).
- [34] J.-J. Wu, R. Molina, E. Oset, and B. S. Zou, *Phys. Rev. C* **84**, 015202 (2011).
- [35] P. Artoisenet, E. Braaten, and D. Kang, *Phys. Rev. D* **82**, 014013 (2010).
- [36] J. A. Oller and E. Oset, *Nucl. Phys.* **A620**, 438 (1997); **A652**, 407(E) (1999).
- [37] E. Oset and A. Ramos, *Nucl. Phys.* **A635**, 99 (1998).
- [38] J. A. Oller and E. Oset, *Phys. Rev. D* **60**, 074023 (1999).
- [39] J. A. Oller and U. G. Meissner, *Phys. Lett. B* **500**, 263 (2001).
- [40] J. A. Oller, E. Oset, and J. R. Pelaez, *Phys. Rev. D* **59**, 074001 (1999); **60**, 099906(E) (1999); **75**, 099903(E) (2007).
- [41] M. B. Voloshin and L. B. Okun, *JETP Lett.* **23**, 333 (1976); *Pis'ma Zh. Eksp. Teor. Fiz.* **23**, 369 (1976).
- [42] N. A. Tornqvist, *Phys. Rev. Lett.* **67**, 556 (1991).
- [43] N. A. Tornqvist, *Phys. Lett. B* **590**, 209 (2004).
- [44] E. S. Swanson, *Phys. Lett. B* **588**, 189 (2004).
- [45] Y.-R. Liu, X. Liu, W.-Z. Deng, and S.-L. Zhu, *Eur. Phys. J. C* **56**, 63 (2008).
- [46] C. E. Thomas and F. E. Close, *Phys. Rev. D* **78**, 034007 (2008).
- [47] E. Braaten, M. Lu, and J. Lee, *Phys. Rev. D* **76**, 054010 (2007).
- [48] S. Fleming, M. Kusunoki, T. Mehen, and U. van Kolck, *Phys. Rev. D* **76**, 034006 (2007).
- [49] M. Suzuki, *Phys. Rev. D* **72**, 114013 (2005).
- [50] V. Baru, A. A. Filin, C. Hanhart, Y. S. Kalashnikova, A. E. Kudryavtsev, and A. V. Nefediev, *Phys. Rev. D* **84**, 074029 (2011).
- [51] R. Molina and E. Oset, *Phys. Rev. D* **80**, 114013 (2009).
- [52] C. Hanhart, Y. S. Kalashnikova, A. E. Kudryavtsev, and A. V. Nefediev, *Phys. Rev. D* **75**, 074015 (2007).
- [53] R. Molina, H. Nagahiro, A. Hosaka, and E. Oset, *Phys. Rev. D* **83**, 094030 (2011).
- [54] L. S. Geng and E. Oset, *Phys. Rev. D* **79**, 074009 (2009).
- [55] D. Gamermann, E. Oset, and B. S. Zou, *Eur. Phys. J. A* **41**, 85 (2009).
- [56] F. S. Navarra, M. Nielsen, and M. E. Bracco, *Phys. Rev. D* **65**, 037502 (2002).
- [57] S.-K. Choi, S. L. Olsen, K. Trabelsi, I. Adachi, H. Aihara, K. Arinstein, D. M. Asner, T. Aushev *et al.*, *Phys. Rev. D* **84**, 052004 (2011).
- [58] J. Beringer *et al.* (Particle Data Group Collaboration), *Phys. Rev. D* **86**, 010001 (2012).